Energy Absorption Capacity of A GRFP Composite under Impact of High Velocity Projectiles

Onyechi, Pius C., Obuka Nnaemeka, S.P., Agbo, Cornelius O., Igwegbe, Chinenye A.

Abstract: In this work, a glass fibre reinforced composite laminates was developed for amour body application. Six samples of this composite laminates were formed with thicknesses of 28mm (Sample E), 24mm (Sample D), 20mm (Sample C), 16mm (Sample B), 12mm (Sample A), and 8mm (Sample F). These samples were targeted using two types of life bullets (Ogival and Conical nosed) moving at a velocity of 355m/s. Energy absorption capacity of these composite laminates was determined as a measure of area under the stress-strain curve through the application of the Simpson's 1/3 rule. Sample E of the GFRP composite gave an optimum absorption energy capacity of 1.956 MJ after ballistic deformation (theoretical) which is greater than the kinetic energies of the conical projectile (456.676 J) and the ogival projectile (348.85 J) obtained from experimental analysis, energy absorption capacities of Samples A-D were also greater then these values. This indicates the ability of the developed composites (Samples A-E) to absorb the projectiles' kinetic energy without perforation.

Keywords: Energy Absorption, GFRP Composite, Ogival and Conical Projectiles, Simpson's 1/3 Rule, Area under Curve, Ballistic Deformation.

1 INTRODUCTION

Fibre reinforced composite laminates are now widely used due to their superiority over metals because of their high stiffness and strength as well as low weight, better corrosion resistance, acoustic and vibrating properties, a high fatigue, crack resistance, impact and explosive shock resistance. A major concern however, about the use of the composite is their low resistance to out-of-plane localized impact loading. A number of works have been reported in the fields of impact phenomenon of fibre reinforced composites materials. Especially, the damage resistance and damage tolerance under impact loading are of the most importance of composite material characteristics because they are often susceptible to impact. Impact on composites is a very complex phenomenon and many parameters influence its analysis.Need exists for high performance, lightweight and cost effective protection for personnel and vehicles to improve impact absorption ability and reduce injury when subjected to a range of threats such as blast and ballistic impacts [1]. The design of composite amour is a very complex task as compared to conventional single layer metallic armour, due to the exhibition of coupling among membrane, torsion and bending strains; weak transverse shear strength, and discontinuity of mechanical properties along the thickness of the composite laminates [2].

- *Onyechi, Pius C., Obuka Nnaemeka, S.P., Agbo, Cornelius .,Igwegbe, Chinenye A*
- *Industrial and Production Engineering Department, Nnamdi Azikiwe University, Awka, Nigeria.*
- *Mechanical/Production Engineering Department, Enugu State University of Science and Technology, Enugu, Nigeria.*
- *Mechanical Engineering Department, University of Nigeria, Nsukka, Nigeria.*
- *Chemical Engineering Department, Nnamdi Azikiwe University, Awka, Nigeria.*
- *Email: silvermeks7777@yahoo.com*

This led to usage of more thick section composites for different applications. Such composite structures undergo different loading conditions during their service life. Impact/ballistic impact is one of the typical loading conditions. Researchers have studied low and high velocity impact of projectiles on composite material targets. Abrate [3]; Cantwell and Morton [4], have reviewed various theories proposed for predicting the characteristics of penetration of composite laminates by different projectiles. Fibre reinforced laminates have been considered for amour application, glass fibre being more popular than other types because of its cost advantage. However, when an impact load is applied to a body, instantaneous stresses are produced, these stresses are not immediately transmitted to all parts of the material. But the remote portions of the material remain undisturbed for a certain period. These stresses propagate in all directions through the material in the form of disturbances of different kinds. This means that stresses and the resultant strains move through the material at specific velocities. These velocities are functions of the material properties. Regardless of the method of application of impact load, the disturbances generated have identical properties based only on the target material properties [5-8]. Al-Hamdan et al [9] put it that low energy impacts are associated with delamination damage in fibre reinforced composite materials, and this inter-laminar debonding primarily may reduce the local bending stiffness and thus can affect the bending and buckling behavior of the structure,by inducing further delamination growth which can lead to overall global weakening of the structure. Nevertheless, energy absorption capacity of any composite material is very critical to improving the human safety during impact, blast or clash. Energy absorption is dependent on many parameters or factors such as type of fibre, matrix type, fibre architecture, specimen geometry, processing conditions, fibre volume fraction, testing speed etc. Changes in these parameters can cause subsequent changes in the specific energy absorption capacity of composite materials [10]. Upon impact, a series of physical phenomena takes place: elastic, shock, and plastic wave propagation, and spallation [11]. Dynamic behaviours of materials focusing on the analysis and design of energy absorbing materials and structures capable of resisting

impact and mitigating blast was presented by [11] and [12]. This paper, therefore, looks into the energy absorption capacity of a novel glass fibre reinforced composite laminates for amour body application impeded with high velocity (ogival and conical nosed) projectiles. The analysis for determining the materials' energy absorption was carried out using the Simpson's 1/3 rule for area under the stress-strain curve.

2 RESEARCH MATERIALS AND METHODOLOGY

2.1 Procedure for the production of the GFRP composite test samples.

The hand lay-up moulding method was used. Here the polyester resin was applied on the mould evenly with the help of a hand brush to a thickness of about 1.5mm [13], then the woven roving fibres were lay-up in the mould and properly wetted out in a process known as fibre impregnation. More fibre plies were lay-up in the mould and compressed according to the required laminate thickness. For the thickness of 28 mm, 24 mm, 20 mm, 16 mm, 12mm and 8mm, the number of plies were 22, 18, 15, 12, 9, and 6 respectively. The fibre content by volume varies from 0.48 to 0.50. At the end of lamination process, the matrixes were allowed to cure for 36 hours. Six composite laminate armour sample plates of size 300mm by 400mm and thicknesses of 8mm, 12mm, 16mm, 20mm, 24mm and 28mm, were targeted using two types of life bullets (Ogival and Conical nosed) of equal diameter and mass. The rifle used was the Beretta Cal 9 x 19 parabellum models 951 of muzzle velocity of 355m/s and the angle of attack was 0^0 (normal). Figs. 1 to 6 show the ballistic impact, penetration and perforation on the six GFRP composite laminate samples.

Fig. 1: Sample E, showing complete absorption of impact.

Fig 2: Sample D, showing minimal shattering by impact.

Fig. 3: Sample C, showing some shattering and penetration, but no perforation.

Fig. 4: Sample B, showing sign of penetration but no perforation.

Fig. 5: Sample A, showing heavy shattering but no perforation

Fig. 6: Sample F, showing failure with complete perforation.

It was observed that five samples (E, D, C, B and A) resisted or arrested the assault of the projectiles while the sixth sample (F) failed (the bullets went through). The distance between the target and the gun was 50meters. The classification of the bullet used is shown in the Table 1.

TABLE 1: CLASSIFICATION OF BULLETS USED [14]

Parameter	Ogival	Conical
Projectile Caliber	22 (5.6 mm)	45^{o} conical tipped
Cartridge size Type	27grain	27grain
Nominal Type	1.7gram	1.7gram
Bullet diameter	5.7mm	5.7mm
Muzzle velocity	355m/s	355m/s
Effective range	200meters	200meters
Mass density of Bullet	11,400kg/m^3	11,400kg/m^3
Length of Bullet	10.7mm	10.7mm
Nose length of Bullet	6.7mm	6.7mm

After the ballistic experiments, the samples were examined. The Ultrasonic thickness measurement/penetration and inspection was carried out on the six GFRP composite samples at BVL Nigeria Limited Port Harcourt, Rivers State, with calibration sensitivity compression-wave and share-wave Scanner. For composite analyzer probe of procedure ASTM E2580-07, the calibration was set at 200mm screen, while the sensitivity was set at 80% full screen height for 1.5mm hole from the calibration block. From Tables 2 and 3, it is observed that the tensile strength of the material before ballistic deformation was 145.833MPa and 97.3MPa after ballistic deformation.

TABLE 2: TENSILE TEST OF COMPOSITE SAMPLE BEFORE BALLISTIC DEFORMATION (STRESS/STRAIN).

A		B		C		D		E	
Stress (MPa)	**Strain**	**Stress (MPa)**	**Strain**	**Stress (MPa)**	**Strain**	**Stress (MPa)**	**Strain**	**Stress (MPa)**	**Strain**
0	0	0	0	0	0	0	0	0	0
40.125	0.0114	14.8	0.0089	17.75	0.0112	27.4	0.0098	24.75	0.0098
64.25	0.0226	27.4	0.0215	35.375	0.0253	46.5	0.022	47.167	0.0233
87.875	0.0351	44.65	0.0348	54.313	0.0363	66.9	0.0327	71.0	0.0341
104.25	0.0446	60.15	0.0438	72.813	0.0463	91.6	0.0423	93.833	0.0426
		76.4	0.0537	89.313	0.0587	111.5	0.0508	116.333	0.0514
		89.15	0.0622	106.5	0.0713	119.26	0.0567	131.117	0.0589
		94.58	0.0776	115.625	0.0803	127.26	0.0617	139.167	0.065
		98.63	0.0881	122.888	0.0889	139.0	0.0641	**145.833**	0.075

TABLE 3: TENSILE TEST OF COMPOSITE SAMPLE AFTER BALLISTIC DEFORMATION (STRESS/STRAIN).

A		B		C		D		E	
Stress (MPa)	**Strain**	**Stress (MPa)**	**Strain**	**Stress (MPa)**	**Strain**	**Stress (MPa)**	**Strain**	**Stress (MPa)**	**Strain**
0	0	0	0	0	0	0	0	0	0
2.632	0.00183	7.407	0.0036	9.09	0.0025	9.868	0.00567	10.81	0.004
5.263	0.00383	14.815	0.0045	18.182	0.0035	19.737	0.008	21.62	0.0055
7.895	0.00517	22.222	0.0052	27.273	0.00433	29.605	0.0095	32.43	0.0075
10.53	0.00633	29.63	0.0058	36.364	0.00533	39.474	0.0112	43.24	0.00883
13.16	0.0073	37.037	0.0065	45.455	0.00617	49.342	0.0125	54.05	0.0102
15.79	0.00817	44.444	0.0072	54.545	0.00717	59.211	0.0142	64.86	0.0113
		51.852	0.0077	63.636	0.0085	69.079	0.0157	75.68	0.0125
		59.259	0.0083	72.727	0.01	78.95	0.0172	86.49	0.0142
		66.667	0.0092	79.1	0.0113	88.816	0.0193	**97.3**	0.0157

2.2 Plots of Stress-Strain Test Results before Deformation

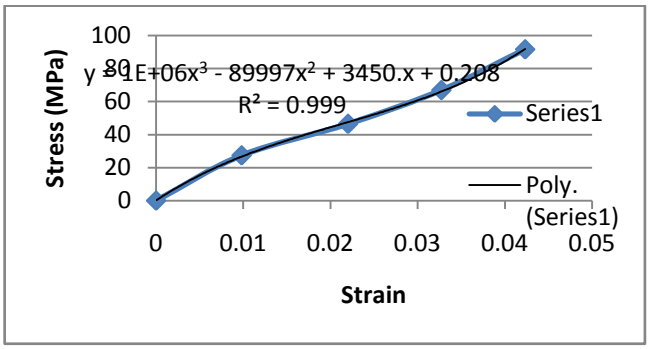

Fig. 7.1(a): Stress-Strain Curve for Sample A

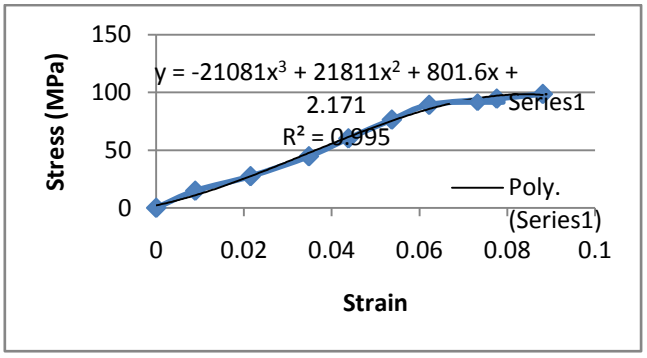

Fig. 7.1(b): Stress-Strain Curve for Sample B

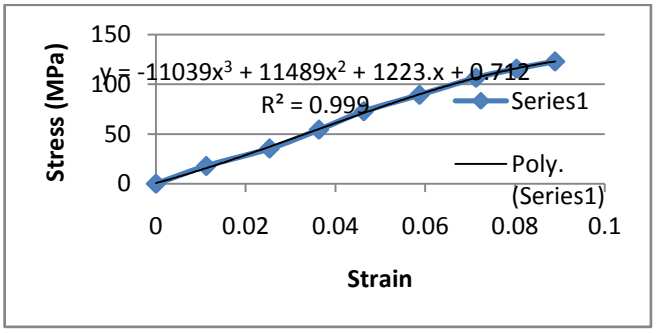

Fig. 7.1(c): Stress-Strain Curve for Sample C

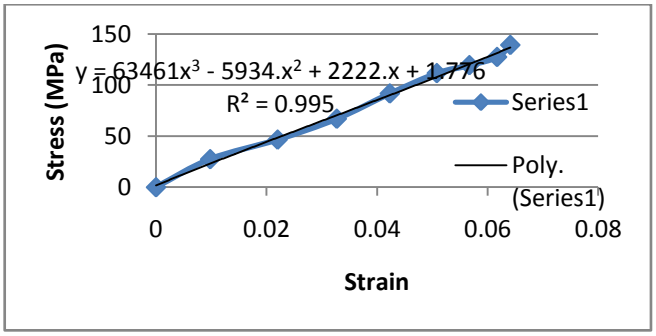

Fig. 7.1(d): Stress-Strain Curve for Sample D

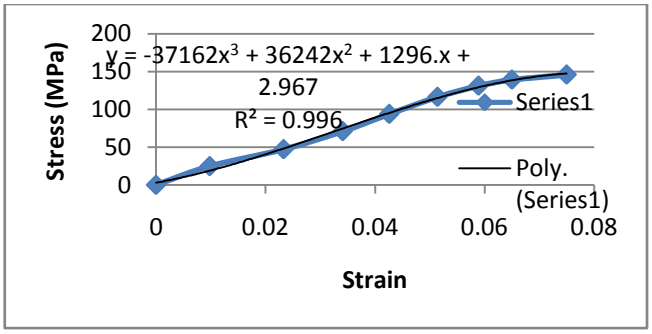

Fig. 7.1(e): Stress-Strain Curve for Sample E

Fig 7.1: Stress - Strain test plots of composite samples before ballistic deformation.

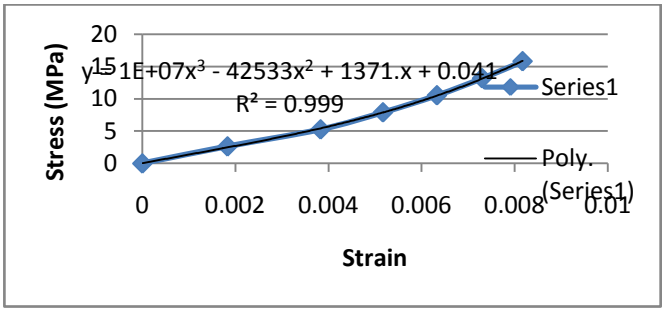

Fig. 7.2(a): Stress-Strain Curve for Sample A

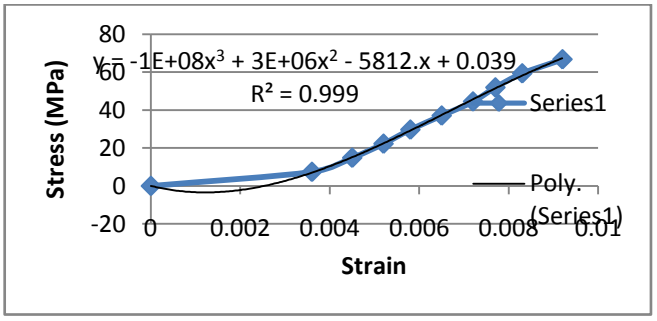

Fig. 7.2(b): Stress-Strain Curve for Sample B

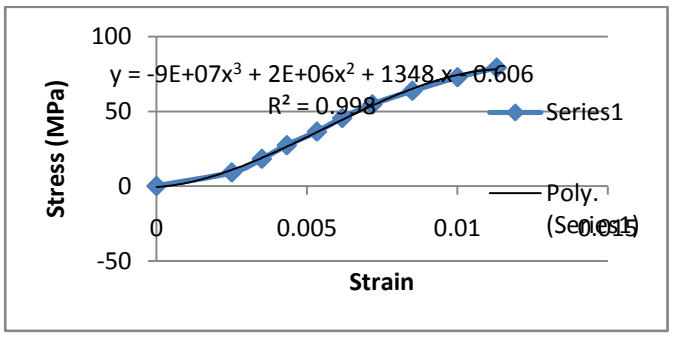

Fig. 7.2(c): Stress-Strain Curve for Sample C

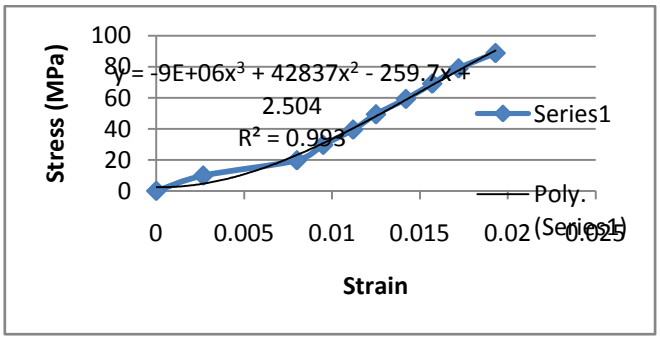

Fig. 7.2(d): Stress-Strain Curve for Sample D

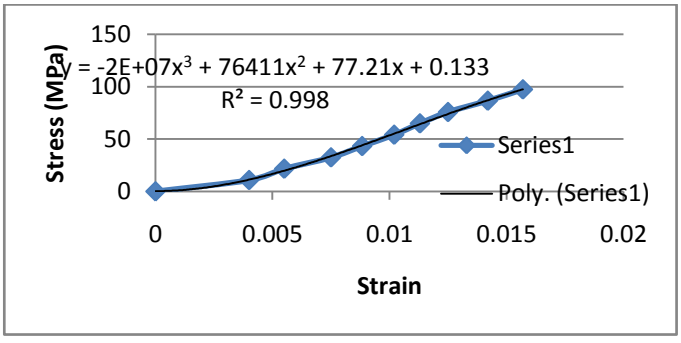

Fig. 7.2(e): Stress-Strain Curve for Sample E

Fig 7.2: Stress - Strain test plots of composite samples after ballistic deformation.

2.3 Energy Absorption Capacity through Area under the Stress-Strain Curve (Simpson's 1/3 Rule)

Energy absorption capacity per unit volume of the GFRP composites developed can be evaluated as a measure of area under the stress-strain curve through the application of the Simpson's 1/3 rule. Tables 2 and 3 were used in plotting the graphs of Figs 7.1(a) – (e) and Figs. 7.2 (a) – (e), hence the areas under these curves were evaluated to estimate energy absorbed by these composite samples before and after ballistic deformation. In order to obtain a more accurate computational estimate of the integral it is better to use higher-order polynomials to connect the points. Therefore third order polynomials were used in defining the trend lines of the curves. Simpson's 1/3 rule results when a second-order or higher interpolating polynomial is substituted into a Newton-Cotes formulas [15];

$$I = \int_a^b f(x)dx \cong \int_a^b f_n(x)dx \qquad (1)$$

Where n is the order of the polynomial, hence after integration and algebraic manipulation of a second-order polynomial the following formula (Simpson's 1/3 rule) results:

$$I \cong \frac{h}{3}[f(x_0) + 4f(x_1) + f(x_2)] \qquad (2)$$

Where $h = \frac{b-a}{n}$ as n is the number of intervals. In order to obtain better results the rule is improved by dividing the integration interval into a number of segments of equal widths and the total integral representing the area under the curve given as;

$$I \cong (b - a)\frac{f(x_0) + 4\sum_{i=1,3,5}^{n-1} f(x_i) + 2\sum_{j=2,4,6}^{n-2} f(x_j) + f(x_n)}{3n} \qquad (3)$$

2.3.1 Computing Absorbed Energy for Composite Samples before Ballistic Deformation

For each of GFRP samples the following numerical evaluation steps were taking in the process of calculating the absorbed energy of the sample from the evaluated area under the stress-strain curve for each sample's plot. Taking for instance sample A, area under stress-strain plot (Fig. 7.1(a)) is divided into four equal segments of eight intervals and each is integrated using equation (1)

For Segment 1A:

$$a = 0, b = 0.01 \; and \; n = 2$$

Therefore;

$$h = \frac{0.01 - 0}{2} = 0.005 \qquad (4)$$

We have our third-order polynomial for Sample A curve given as;

$$f(x) = 1000000x^3 - 89997x^2 + 3450x + 0.208 \qquad (5)$$

Hence applying (5) we obtain the values of f(x) at this segment as follows;

$$\left.\begin{array}{l} f(x_0) = f(0.000) = 0.208 \\ f(x_1) = f(0.005) = 15.333 \\ f(x_2) = f(0.01) = 26.708 \end{array}\right\} \qquad (6)$$

Computing the values of (6) into (2) we have;

$$I = 0.005\frac{[0.208 + (4 \times 15.333) + 26.708]}{3} = 0.147 \; J/mm^3$$

For Segment 2A:

$$a = 0.01, b = 0.02 \; and \; n = 2$$

Therefore;

$$h = \frac{0.02 - 0.01}{2} = 0.005 \qquad (7)$$

Hence applying (7) we obtain the values of f(x) at this segment as follows;

$$\left.\begin{array}{l} f(x_2) = f(0.01) = 26.708 \\ f(x_3) = f(0.015) = 35.083 \\ f(x_4) = f(0.02) = 41.209 \end{array}\right\} \qquad (8)$$

Computing the values of (8) into (2) we have;

$$I = 0.005\frac{[26.708 + (4 \times 35.083) + 41.209]}{3} = 0.3471 \; J/mm^3$$

For Segment 3A:

$$a = 0.02, b = 0.03 \; and \; n = 2$$

Therefore;

$$h = \frac{0.03 - 0.02}{2} = 0.005 \qquad (9)$$

Hence applying (7) we obtain the values of f(x) at this segment as follows;

$$\left.\begin{array}{l} f(x_4) = f(0.02) = 41.209 \\ f(x_5) = f(0.025) = 45.835 \\ f(x_6) = f(0.03) = 49.711 \end{array}\right\} \qquad (10)$$

Computing the values of (10) into (2) we have;

$$I = 0.005\frac{[41.209 + (4 \times 45.835) + 49.711]}{3} = 0.4571 \; J/mm^3$$

For Segment 4A:

$$a = 0.03, b = 0.04 \; and \; n = 2$$

Therefore;

$$h = \frac{0.04 - 0.03}{2} = 0.005 \qquad (11)$$

Hence applying (7) we obtain the values of f(x) at this segment as follows;

$$\left.\begin{array}{l} f(x_6) = f(0.03) = 49.711 \\ f(x_7) = f(0.035) = 53.587 \\ f(x_8) = f(0.04) = 58.213 \end{array}\right\} \qquad (12$$

Computing the values of (12) into (2) we have;

$$I = 0.005\frac{[49.711 + (4 \times 53.587) + 58.213]}{3} = 0.537\, J/mm^3$$

Therefore total integral which is the area under the curve for the plot of Sample A is given by the summation of individual integral segment, as expressed by equation (3) is obtained as;

$\text{Total I} = 0.147 + 0.3471 + 0.4571 + 0.537 = \mathbf{1.488\ J/mm^3}$
Converting to Joule we have
$1.488 \times \text{vloume of sample} = 2{,}142{,}720\ \text{J} = \mathbf{2.143\ MJ}$

Following the same algebraic processes the parametric values and energy absorbed by Samples A to E is evaluated, and values shown in Tables 4 (a to e) and Table 5 respectively.

TABLE 4: PARAMETRIC VALUES FOR AREA UNDER CURVE OF SAMPLES BEFORE BALLISTIC DEFORMATION.

a. Sample A with $f(x) = 1000000x^3 - 89997x^2 + 3450x + 0.208$

SEGMENT 1					
a	b	H	$f(x_0)$	$f(x_1)$	$f(x_2)$
0.00	0.01	0.005	0.208	15.333	26.708
SEGMENT 2					
a	b	H	$f(x_2)$	$f(x_3)$	$f(x_4)$
0.01	0.02	0.005	26.708	35.083	41.209
SEGMENT 3					
a	b	H	$f(x_4)$	$f(x_5)$	$f(x_6)$
0.02	0.03	0.005	41.209	45.835	49.711
SEGMENT 4					
a	b	H	$f(x_6)$	$f(x_7)$	$f(x_8)$
0.03	0.04	0.005	49.711	53.587	58.213

b. Sample B with $f(x) = -21081x^3 + 21811x^2 + 801.6x + 2.171$

SEGMENT 1					
a	b	H	$f(x_0)$	$f(x_1)$	$f(x_2)$
0.00	0.02	0.01	2.171	12.347	26.758
SEGMENT 2					
a	b	H	$f(x_2)$	$f(x_3)$	$f(x_4)$
0.02	0.04	0.01	26.758	45.280	67.784
SEGMENT 3					
a	b	H	$f(x_4)$	$f(x_5)$	$f(x_6)$
0.04	0.06	0.01	67.784	94.144	124.251
SEGMENT 4					
a	b	H	$f(x_6)$	$f(x_7)$	$f(x_8)$
0.06	0.08	0.01	124.251	157.926	195.095

c. Sample C with $f(x) = -11039x^3 + 11489x^2 + 1223x + 0.712$

SEGMENT 1					
a	b	H	$f(x_0)$	$f(x_1)$	$f(x_2)$
0.00	0.02	0.01	0.712	14.080	29.680
SEGMENT 2					
a	b	H	$f(x_2)$	$f(x_3)$	$f(x_4)$
0.02	0.04	0.01	29.680	47.444	67.307
SEGMENT 3					
a	b	H	$f(x_4)$	$f(x_5)$	$f(x_6)$
0.04	0.06	0.01	67.307	89.205	113.068
SEGMENT 4					
a	b	H	$f(x_6)$	$f(x_7)$	$f(x_8)$
0.06	0.08	0.01	113.068	138.832	166.430

d. Sample D with $f(x) = 63461x^3 - 5934x^2 + 2222x + 1.776$

SEGMENT 1					
a	b	H	$f(x_0)$	$f(x_1)$	$f(x_2)$
0.01	0.03	0.01	23.470	44.373	64.811
SEGMENT 2					
a	b	H	$f(x_2)$	$f(x_3)$	$f(x_4)$
0.03	0.05	0.01	64.811	85.227	105.977
SEGMENT 3					
a	b	H	$f(x_4)$	$f(x_5)$	$f(x_6)$
0.05	0.07	0.01	105.977	127.443	150.009
SEGMENT 4					
a	b	H	$f(x_6)$	$f(x_7)$	$f(x_8)$
0.07	0.09	0.01	150.009	174.053	199.957

e. Sample E with $f(x) = -37162x^3 + 36242x^2 + 1296x + 2.967$

SEGMENT 1					
a	b	H	$f(x_0)$	$f(x_1)$	$f(x_2)$
0.00	0.02	0.01	2.967	19.514	43.087
SEGMENT 2					
a	b	H	$f(x_2)$	$f(x_3)$	$f(x_4)$
0.02	0.04	0.01	43.087	73.461	110.416
SEGMENT 3					
a	b	H	$f(x_4)$	$f(x_5)$	$f(x_6)$
0.04	0.06	0.01	110.416	153.727	203.171
SEGMENT 4					
a	b	H	$f(x_6)$	$f(x_7)$	$f(x_8)$
0.06	0.08	0.01	203.171	258.526	319.569

TABLE 5: ENERGY ABSORPTION DATA FOR SAMPLES BEFORE BALLISTIC DEFORMATION

	Area of Seg. 1 (J/mm^3)	Area of Seg. 2 (J/mm^3)	Area of Seg. 3 (J/mm^3)	Area of Seg. 4 (J/mm^3)	Energy Absorbed = ΣArea of Segments	
					(J/mm^3).	MJ
Sample A	0.147	0.3471	0.4571	0.537	**1.488**	**2.143**
Sample B	0.261	0.919	1.895	3.170	**6.20**	**11.904**
Sample C	0.289	0.956	1.791	2.783	**5.819**	**13.966**
Sample D	0.886	1.706	2.553	3.487	**8.632**	**24.860**
Sample E	0.414	1.491	3.095	5.190	**10.19**	**34.238**

2.3.2 Computing Absorbed Energy for Composite Samples after Ballistic Deformation

Following the same algebraic processes as samples before ballistic deformation, the energy absorption capacity of the GFRP composites was evaluated and the result shown in Table 6 (a to e) and Table 7.

TABLE 6: PARAMETRIC VALUES FOR AREA UNDER CURVE OF SAMPLES AFTER BALLISTIC DEFORMATION.

a. Sample A with $f(x) = 10000000x^3 - 42533x^2 + 1371x + 0.041$

SEGMENT 1					
a	b	H	$f(x_0)$	$f(x_1)$	$f(x_2)$
0.00	0.002	0.001	0.041	1.379	2.693
SEGMENT 2					
a	b	H	$f(x_2)$	$f(x_3)$	$f(x_4)$
0.002	0.004	0.001	2.693	4.041	5.484
SEGMENT 3					
a	b	H	$f(x_4)$	$f(x_5)$	$f(x_6)$
0.004	0.006	0.001	5.484	7.083	8.896
SEGMENT 4					
A	b	H	$f(x_6)$	$f(x_7)$	$f(x_8)$
0.006	0.008	0.001	8.896	10.984	13.407

b. Sample B with $f(x) = -100000000x^3 + 3000000x^2 + 5812x + 0.039$

SEGMENT 1					
A	b	H	$f(x_0)$	$f(x_1)$	$f(x_2)$
0.00	0.002	0.001	0.039	-2.873	-0.385
SEGMENT 2					
A	b	H	$f(x_2)$	$f(x_3)$	$f(x_4)$
0.002	0.004	0.001	-0.385	6.903	18.391
SEGMENT 3					
A	b	H	$f(x_4)$	$f(x_5)$	$f(x_6)$
0.004	0.006	0.001	18.391	33.479	51.567
SEGMENT 4					
A	b	H	$f(x_6)$	$f(x_7)$	$f(x_8)$
0.0006	0.08	0.001	51.567	72.055	94.343

c. Sample C with $f(x) = -90000000x^3 + 2000000x^2 + 1348x - 0.606$

SEGMENT 1					
A	b	H	$f(x_0)$	$f(x_1)$	$f(x_2)$
0.00	0.004	0.002	-0.606	9.370	31.026
SEGMENT 2					
A	b	H	$f(x_2)$	$f(x_3)$	$f(x_4)$
0.004	0.008	0.002	31.026	60.042	92.080
SEGMENT 3					
A	b	H	$f(x_4)$	$f(x_5)$	$f(x_6)$
0.008	0.012	0.002	92.080	122.874	148.050

d. Sample D with $f(x) = -9000000x^3 + 42837x^2 - 259.7x + 2.504$

SEGMENT 1					
A	b	H	$f(x_0)$	$f(x_1)$	$f(x_2)$
0.00	0.005	0.0025	2.504	1.982	1.151
SEGMENT 2					
A	b	H	$f(x_2)$	$f(x_3)$	$f(x_4)$
0.005	0.01	0.0025	1.151	-0.831	-4.809
SEGMENT 3					
A	b	H	$f(x_4)$	$f(x_5)$	$f(x_6)$
0.01	0.015	0.0025	-4.809	-11.631	-22.129
SEGMENT 4					
A	b	H	$f(x_6)$	$f(x_7)$	$f(x_8)$
0.015	0.02	0.0025	-22.129	-37.156	-52.555

e. Sample E with $f(x) = -20000000x^3 + 76411x^2 + 77.21x + 0.133$

SEGMENT 1					
A	b	H	$f(x_0)$	$f(x_1)$	$f(x_2)$
0.00	0.005	0.0025	0.133	0.491	-0.071
SEGMENT 2					
A	b	H	$f(x_2)$	$f(x_3)$	$f(x_4)$
0.005	0.01	0.0025	-0.071	-3.428	-11.454
SEGMENT 3					
A	b	H	$f(x_4)$	$f(x_5)$	$f(x_6)$
0.01	0.015	0.0025	-11.454	-26.026	-49.016
SEGMENT 4					
A	b	H	$f(x_6)$	$f(x_7)$	$f(x_8)$
0.015	0.02	0.0025	-49.016	-82.303	-127.759

TABLE 7: ENERGY ABSORPTION DATA FOR SAMPLES AFTER BALLISTIC DEFORMATION

	Area of Seg. 1 (J/mm^3)	Area of Seg. 2 (J/mm^3)	Area of Seg. 3 (J/mm^3)	Area of Seg. 4 (J/mm^3)	Energy Absorbed = ΣArea of Segments	
					(J/mm^3).	MJ
Sample A	0.00275	0.00811	0.014	0.022	**0.047**	**0.068**
Sample B	-0.00395	0.0152	0.068	0.145	**0.232**	**0.445**
Sample C	0.0453	0.242	0.488	-	**0.775**	**1.860**
Sample D	0.00965	-0.0058	-0.0612	-0.186	**0.263**	**0.757**
Sample E	0.00169	-0.021	-0.137	-0.422	**0.582**	**1.956**

2.4 Ballistic Test Results

The equations formulated in literatures [16] were computed with the experimental data for indentation, penetration and perforation of GFRP laminate target samples by the rigid conical and ogival nosed projectiles. The values of the parameter (β) in the equations have been empirically determined and are taken to be 2sinθ/2 and 3/(4Ψ) for conical-nosed and ogival-nosed projectiles respectively [16]. The values of these computations serve as the experimental ballistic test results as tabulated in Tables 8 and 9.

2.4.1 Conical Nose Projectile

TABLE 8: RESULTS OBTAINED IN CONICAL PROJECTILE ANALYSIS

t[mm]	d_p [mm]	t/D	E_k [J]	V_b [m/s]	E_b [J]	V_r
0	0	0	0	0	0	355
1	1	0.175439	0.012225163	32.57527	4.033387	322.4247
2	2	0.350877	0.391205221	65.14829	8.690893	289.8517
3	3	0.526316	2.970714647	97.72131	13.97252	257.2787
4	4	0.701754	12.51856707	130.2943	19.87826	224.7057
5	5	0.877193	38.20363487	162.8674	26.40812	192.1326
6	6	1.052632	95.06286872	195.4404	33.5621	159.5596
7	7	1.22807	82.1558888	228.0134	41.3402	126.9866
8	8	1.403509	116.2031682	260.5864	49.74242	94.41358
9	9	1.578947	150.2504476	293.1594	58.76875	61.84056
10	10	1.754386	184.297727	325.7325	68.41921	29.26754
12	11	2.105263	218.3450064	390.8785	89.59248	-35.8785*
16	13.5	2.807018	303.4632049	521.1706	139.4284	-166.171*
20	16	3.508772	388.5814034	651.4627	199.2503	-296.463*
24	17	4.210526	422.6286828	781.7548	269.058	-426.755*
28	18	4.912281	456.6759622	912.0468	348.8517	-557.047*

***Theoretical values of Residual velocities.

2.4.2 Ogival-Nosed Projectile

TABLE 9: RESULTS OBTAINED IN OGIVAL PROJECTILE ANALYSIS

t[mm]	d_p [mm]	T/D	F [N]	E_k [J]	V_b [m/s]	E_b [J]	V_r
0	0	0	0	0	0	0	355
1	1	0.175439	0.071887	0.901187	32.56103	4.033114	322.439
2	2	0.350877	0.287549	3.604501	65.1198	8.689801	289.8802
3	3	0.526316	0.646985	8.10994	97.67858	13.97006	257.3214
4	4	0.701754	1.150195	14.4175	130.2374	19.87389	224.7626
5	5	0.877193	1.79718	22.5272	162.7961	26.4013	192.2039
6	6	1.052632	2.587939	32.44901	195.3549	33.55228	159.6451
7	7	1.22807	3.403241	49.7436	227.9137	41.32683	127.0863
8	8	1.403509	3.403241	68.4203	260.4725	49.72496	94.52752
12	10	2.105263	3.403241	89.59133	390.7076	89.55319	-35.7076*
16	12	2.807018	3.403241	139.4320	520.9427	139.3586	-165.943*
20	14	3.508772	3.403241	199.2544	651.1778	199.1412	-296.178*
24	15.5	4.210526	3.403241	269.0629	781.4129	268.9009	-426.413*
28	16	4.912281	3.403241	348.8513	911.6481	348.6378	-556.648*

*Theoretical values of Residual velocities.

3. DISCUSSION OF RESULTS

Experimental and analytical investigation have been performed concerning the static and ballistic resistance of woven roving GFRP laminate plates of thicknesses 8mm up to 28mm penetrated and perforated by ogival and conical projectiles. The theoretical analysis of the stress-strain parameter which is the major determinant of the ultimate strength of the developed composites was carried out by determining the energy absorption capacity of the composite materials. Analytical investigation into the areas under the stress-strain curves of Figs. 7.1a-e and Figs.7.2a-e show the following;

a) Sample E has the absorbed energy at the ultimate strength of the composite at the value of 34.238 MJ. Table 5 gives the values for all samples at ultimate strength of each.

b) Sample E also has the optimal absorption energy capacity after ballistic deformation, though sample C showed an arbitrarily high absorbed energy at this instant, but this value did not conform to its absorbed energy at ultimate strength.

c) From Table 7, all samples (A-E) showed absorbed energies after ballistic deformations which are greater than the ballistic energy values of the composite samples observed from the experimental data of Table 8 (Conical projectile) and Table 9 (Ogival) valued at 348.852 J and 348.638 J respectively.

d) The GFRP composite (Sample E) gave an optimum absorbed energy of 1.956 MJ after ballistic deformation (theoretical) which is greater than the kinetic energies of the conical projectile (456.676 J) and the ogival projectile (348.85 J) obtained from experimental analysis, samples A-D were also greater then these values. This indicates the ability of the developed composites (Samples A-E) to absorb the projectiles' kinetic energy without perforation.

4. CONCLUSION

The theoretical analysis of the energy absorption capacity of the developed GFRP composite laminates through the application of Simpson's 1/3 rule to evaluate the area under the stress-strain curve as a measure of absorbed energy clearly shows that the composite materials developed (Samples A-E) were able to absorb the projectiles' (conical and ogival nosed) kinetic energy.

5. REFERENCES

[1] Onyechi, P.C., Edelugo, S.O., Ihueze, C.C., Obuka, S.P.N., and Chukwumuanya, E.O. (2013). High Velocity Impact Response Evaluation of a Glass Fibre Reinforced Polymer (GFRP) Composite: Amour Body. International Journal of Energy Engineering, Vol. 3, No. 5, Pp 242-255.

[2] Patel, B.P., Bhola, S.K., Gamapathi, M., and Makhecha, D.P. (2004). Penetration of Projectiles in Composite Laminates. Defense Science Journal, Vol.54, No. 2, Pp151-159.

[3] Abrate, S. (1994). Impact on Laminated Composites: Recent Advances. Application Mechanics Review, Vol. 47, Pp 517-544.

[4] Cantwell, W.J., and Morton, J. (1991). The Impact Resistance of Composite Materials: A Review. Composites, Vol. 22, Pp 347-362.

[5] Naik, N.K., and Doshi, A.V. (2008). Aerospace Engineering Department, Indian Institute of Technology, Bombay, Powai, Mumdai 400 076.

[6] Naik, N.K., and Shrirao, P. (2004). Composite Structures Under Ballistic Impact Composite Structures, Vol. 66. Pp 570-590.

[7] Naik, N.K., Shrirao, P., and Reddy, B.C.K. (2005). Ballistic Impact Behaviour of Woven Fabric Composites: Parametric Studies Material Science Engineering A, Vol. 412, Pp 104-116.

[8] Naik, N.K., Shrirao, P., and Reddy, B.C.K. (2006). Ballistic Impact Behaviour of Woven Fabric Composites: Formulation. International Journal of Impact Engineering, Vol. 32, Pp 1521-1552.

[9] Al-Hamdan, A., Yassin, L.N., and Ramadan, J.M. (2010). Ballistic Impact Fracture Behaviour of Continuous Fibre Reinforced Al-Matrix Composites, Vol. 4, No. 5, Pp 605-614.

[10] Jacob, G.C. Fellers, J.F., Simunovk, S., and Sarbuck, J.M. (2002). Energy Absorption in Polymer Composites for Automotive Crashworthiness. Journal of Composite Materials, Vol. 36, No. 7, Pp 813-850.

[11] Meyers, M.A. (1994). Dynamic Behaviour of Materials, Wiley, New York.

[12] Nesterenko, V.F. (2001). Dynamics of Heterogeneous Materials, Springer, New York.

[13] Wood, R. (1980). Car Body in Glass Reinforced Plastic. Pentech Press Limited, London, pp 43 - 45.

[14] Cartridges of the World (.22 caliber). http://www.wikipedia.com/.22 short.

[15] Chapra, S.C., and Canale, R.P. (2008). Numerical Methods for Engineers. 5th Ed. McGraw Hill Publishers, India. Pp 478-496.

[16] Wen, H.M. (2000). Predicting the Penetration & Perforation of FRP Laminates Struct Normally by Projectiles with Different Nose Shapes. Composite Structures, 49, 321 –329.